Pulsatile Movement of the Optic Nerve Head and the Peripapillary Retina in Normal Subjects and in Glaucoma

Kanwarpal Singh,[1–3] *Carolyne Dion,*[2,3] *Antoine G. Godin,*[2,4] *Faezeh Lorghaba,*[2,5] *Denise Descovich,*[2] *Marcelo Wajszilber,*[2] *Tsuneyuki Ozaki,*[2,3] *Santiago Costantino,*[1,2,5] *and Mark R. Lesk*[1,2]

Purpose. To measure the pulsatile movement of neuroretinal tissue at the optic nerve head synchronous with the cardiac cycle.

Methods. We used a noninvasive imaging device based on Fourier domain low-coherence interferometry to measure the pulsatile movements of the optic nerve head, peripapillary retina, and cornea with submicron accuracy along a line across the fundus. We also measured the change in the Axial Distance between the peripapillary Retina and the base of the optic disc Cup (ADRC) during the cardiac cycle. Twelve normal subjects and 20 subjects with open-angle glaucoma were tested.

Results. In normal subjects, the mean fundus pulsation amplitude (defined as the fundus movement minus the simultaneous corneal movement) were 13.0 ± 2.5 μm, 9.0 ± 2.1 μm, and 8.7 ± 2.9 μm at the base of the optic nerve head cup, the nasal peripapillary retina, and the temporal peripapillary retina, respectively, compared with 16.7 ± 6.8 μm, 17.3 ± 10.9 μm, and 12.7 ± 6.2 μm for the corresponding values in the glaucoma group ($P = 0.26$, $P = 0.008$, and $P = 0.12$, respectively). The mean changes in ADRC during the cardiac cycle in normal subjects were 10.7 ± 2.1 μm and 11.6 ± 1.8 μm for the nasal and temporal side of the optic disc, respectively, compared to 14.9 ± 5.6 μm and 14.0 ± 4.9 μm in glaucoma subjects ($P = 0.03$ and $P = 0.10$, respectively).

Conclusions. There was an approximately 11-μm pulsatile change in the ADRC in normal subjects, and on the nasal side of the disc, this amount was significantly greater in glaucoma patients. (*Invest Ophthalmol Vis Sci.* 2012;53:7819–7824) DOI:10.1167/iovs.12-9834

While there has been considerable progress in recent decades,[1,2] the mechanism of axonal damage in glaucoma is not fully understood. Clinical, epidemiological,[3] experimental, and mathematical modeling data[4] suggest that factors such as intraocular pressure (IOP), low ocular perfusion pressure, age, ethnicity, greater scleral elasticity, and myopia contribute to the development of glaucoma; however, it is not known how, mechanistically, such factors might combine to cause the pattern of axonal loss and optic disc morphological change that clinicians recognize as glaucoma.

We hypothesized that the pulsatility of the ocular fundus might contribute to axonal damage and loss of the retinal nerve fiber layer in glaucoma. This hypothesis was based on several observations. First, ocular pulsatility increases with increasing IOP,[5,6] as well as with decreasing ocular perfusion pressure,[7] two of the major risk factors for glaucoma.[8] Secondly, choroidal filling during systole (the major source of fundus pulsations) results in a forward displacement of the overlying retina but may also cause an expansion of the corneal-scleral shell of the eye.[7,9] Extrapolating to the area of the optic nerve head (ONH), it is possible that in systole, the retina and the lamina cribrosa (as a continuation of the surrounding sclera) move in opposite directions, leading to deformation and even stretching of axons running into the ONH.

In order to test this hypothesis, we developed a noninvasive imaging device based on Fourier domain low-coherence interferometry (FD-LCI) which measures the position of the cornea, retinal surface, and ONH simultaneously with high spatial and temporal resolution.[9] Here, we report the application of this device to measure the pulsatile movement of these tissues in normal subjects and in open-angle glaucoma patients.

Methods

In this study, we recruited 12 normal healthy volunteers and 20 subjects with open-angle glaucoma. The experiments were approved by the ethics committee of Maisonneuve-Rosemont Hospital, Montreal. All volunteers were informed about the procedure, and written consent was obtained after explaining the consequences of the study. All subjects were treated in accordance with the Declaration of Helsinki. Before the measurements were taken, all the subjects underwent a standard eye exam. If both eyes were eligible then the study eye was chosen randomly. Measurements for IOP, axial length, and blood pressure were taken. Age-matched normal subjects that were recruited either had early cataracts or were accompanying glaucoma patients. They had normal eye exams (except possibly a nonsignificant cataract), including normal IOPs, normal optic discs,

From the [1]Department of Ophthalmology, Faculty of Medicine, Université de Montreal, Montréal, Quebec, Canada; the [2]Centre de Recherche de l'Hôpital Maisonneuve-Rosemont, Montreal, Quebec, Canada; the [3]Institut National de la Recherche Scientifique-Énergie Matériaux Télécommunications, Varennes, Quebec, Canada; the [4]Institut Universitaire en Santé Mentale de Quebec, Quebec, Quebec, Canada; and the [5]Biomedical Engineering Institute, Université de Montreal, Montreal, Quebec, Canada.

Supported by the Ministère du Développement Économique de l'Innovation et de l'Exportation du Quebec, the Fonds Québécois de la Recherche sur la Nature et les Technologies, the Natural Sciences and Engineering Research Council of Canada, the Canadian Institutes of Health Research, the Fonds de la Recherche en Santé du Quebec, the Fonds de Recherche en Ophtalmologie de Universite de Montreal, the Canadian Glaucoma Clinical Research Council of the Canadian National Institute for the Blind, and the Canadian Institute for Photonic Innovations.

Submitted for publication March 10, 2012; revised August 29 and October 18, 2012; accepted October 22, 2012.

Disclosure: **K. Singh**, None; **C. Dion**, None; **A.G. Godin**, None; **F. Lorghaba**, None; **D. Descovich**, None; **M. Wajszilber**, P; **T. Ozaki**, P; **S. Costantino**, None; **M.R. Lesk**, P

Corresponding author: Mark R. Lesk, Ophthalmology, HMR, 5415 Boul L'Assomption, Montreal, Quebec, Canada H1T 2M4; lesk@videotron.ca.

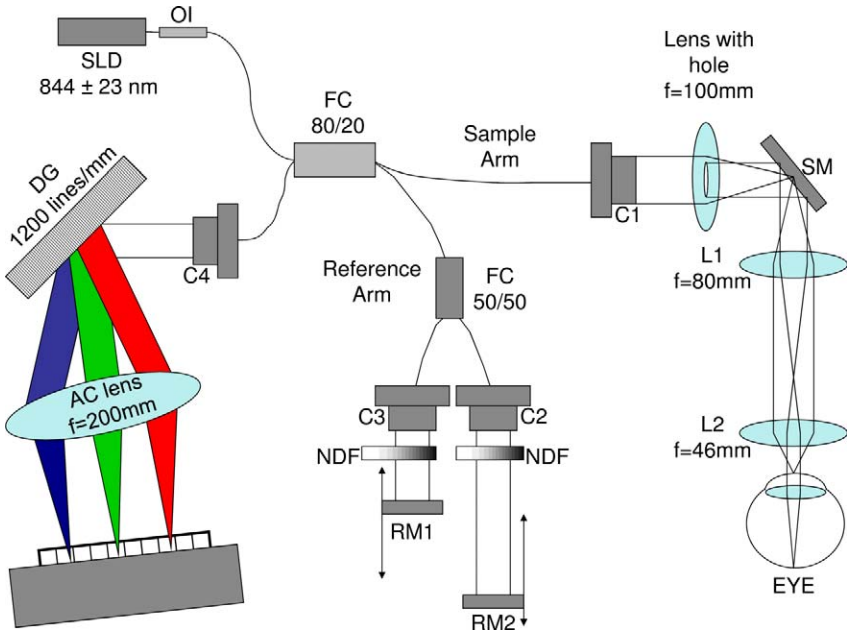

Figure 1. Layout of the optical system. Different components are the superluminescent diode (SLD), optical isolator (OI), fiber coupler (FC), collimator (C1-C4), lens (L1-L2) with focal length (f), scanning mirror (SM), reference mirror (RM1-RM2), neutral density filter (NDF), dispersion grating (DG), and achromatic (AC) lens.

and normal fundus. Patients included in the glaucoma group had medically treated open-angle glaucoma, typical glaucomatous optic nerves, and typical glaucomatous visual field defects without other eye disease and had not had incisional ocular surgery.

Experimental Setup

Our optical system was based on FD-LCI. The theoretical aspects of FD-LCI have been explained elsewhere.[9,10] The schematic of the optical system used in this study is shown in Figure 1 and has been described in detail in our previous work.[9] Briefly, a superluminescent diode (844 ± 23 nm wavelength) was used as a light source and coupled to a fiber-based Michelson interferometer. Light from the superluminescent diode was split into the reference and sample arms using a 2 × 2, 80:20 fiber coupler. In the sample arm, a collimator was used to produce a 3-mm-diameter beam. The light beam from the sample arm was passed through a lens ($f = 100$ mm) with a central hole of 2 mm in diameter. This configuration generated two signals, the focusing outer part of the beam and the parallel central part of the beam. After the scanning optics, the outer part of the sample beam was stationary and focused on the cornea, whereas the collimated central part was scanned and focused at the retina. With this scheme, we were able to obtain the reflected signals from the corneal apex and fundus simultaneously. In the reference arm, a 2 × 1, 50:50 fiber coupler was used to obtain two reference signals. These reference signals were reflected by mirrors mounted on separate motorized translation stages (Zaber Technology, Vancouver, Canada). A neutral density filter was used in the reference arm to keep the total intensity at the camera below the saturation level. The combined reflected signal from the reference arm and the sample arm were dispersed using a reflective diffraction grating (1200 lines/mm). The dispersed signal was focused by an achromatic lens ($f = 200$ mm) on a linear charge-coupled device (CCD) camera (Spyder 3; Dalsa Technology, Waterloo, Canada). In order to simultaneously measure the pulse during the data collection, we used a custom-made oximeter based on hemoglobin saturation[11] which measured the transmission of the infrared light signal through the tissue. The pulse was acquired at the earlobe of the subject and transferred to the computer using a data acquisition card (Labjack, Lakewood, CO). The reader should note that although there is a delay between the ear pulse and ocular pulse, we used the pulse monitor only to obtain the cardiac frequency through Fourier transforming the cardiac pulsation data. The collected data were processed with custom software (LabView; National Instruments, Austin, TX).

Data Analysis

The methodology for the data analysis for this publication is an extension of what has been detailed in our previous works.[9,10] The analysis was performed using MatLab routines (MathWorks Corporation, Natick, MA). Briefly, in order to obtain the axial scans (A-scans) containing positional information, we calculated the fast Fourier transforms (FFT) of the recorded interferograms at the linear CCD camera. For every image, each A-scan was laterally averaged with its 2 closest neighbors. To measure movement of the inner retina, the user delimitated approximately the inner retina and base of the cup (magenta mask in Fig. 2B). A precise delimitation of the inner retina is not required since the mask is automatically copied throughout the image series and because we are looking at change of retinal position rather than absolute position. In order to assign a position to the inner retina, in each A-scan, the intensity centroid was calculated in one dimension but only considering the pixels of the mask of the inner retina. The centroid was then computed by using the formula $\sum X_n I_n^4 / \sum I_n^4$, where X_n is the position of the nth pixel and I_n is its intensity. The fourth exponent was used to reduce the noise contribution. Examples of the retinal positions obtained for two images from the same movie are shown in Figures 2C and 2D. To correct for lateral eye movements, the user provided, for each movie, a large mask (blue mask in Fig. 2B) delimiting the entire retina for the first frame of the movie. Then, for each frame time, the large mask was moved automatically in order to maximize the intensity enclosed in this mask. The whole retinal centroid position was calculated using the same formula as above. This process was repeated automatically for each frame time. We used the first frame as a reference, and using a least squared algorithm, we found the lateral shift that minimized the difference between those two retinal positions. This lateral shift correction algorithm was applied to all images, and an example of the

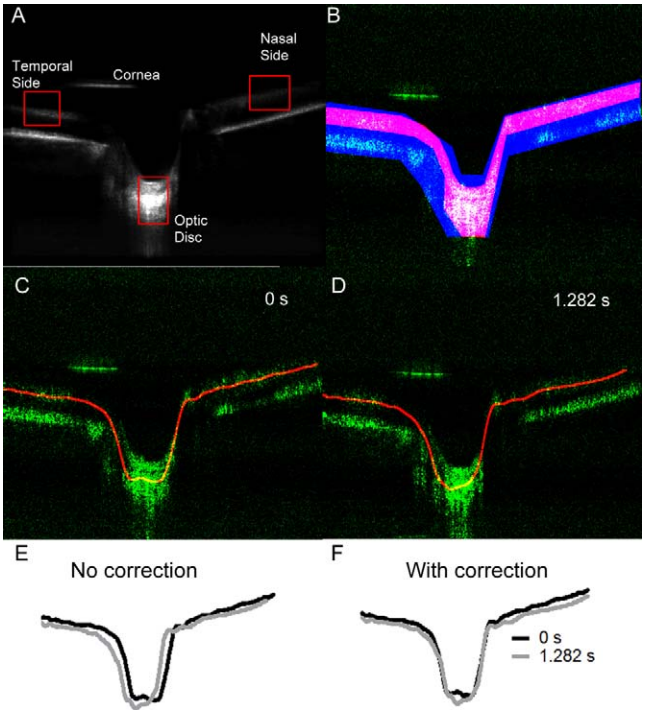

Figure 2. (**A**) Different measurement points in the B-scan of the eye are shown. The optical path lengths of the reference mirrors were adjusted in order to bring the B-scans of the cornea and the retina into the same scan. For illustration purposes only, 100 scans were averaged after being corrected for lateral and axial shifts as explained in the text. (**B**) Example of the segmentation dividing the image. The internal retinal/base of cup mask used to determine axial positions is shown in *magenta*, while the mask of the entire retina used to measure the lateral shift is shown in *blue*. (**C**, **D**) Images at two different times with the centroid of the magenta mask shown in *red*. The raw centroid positions of the images presented in (**C**, **D**) are shown in (**E**) and the centroid positions corrected for lateral shift with time = 0 as reference are shown in (**F**).

correction for two images of the same movie is shown in Figures 2E and 2F.

For a given shift-corrected time series, out of the total scan length of approximately 4.7 mm over the retina, three regions (approximately 100 μm long) within the scan were manually indicated as the nasal and temporal peripapillary retina and the base of the optic disc cup. The nasal and the temporal areas were selected close to the rim of the optic disc in order to measure the tissue deformation in optic disc area. The A-scans included in these regions were used to calculate their intensity centroids, and these positions were averaged to assign one location to each region (cornea, nasal retina, temporal retina, and optic disc) for every frame. These centroids are representative of the entire inner retina or the entire base of the cup rather than the centroids of any individual retinal layer. The position of the corneal epithelium at the apex was also calculated simultaneously for each image in a similar manner. To calculate the change in distance between two tissues over time, the position averaged over the selected regions of the two tissues is subtracted at each time point.

The root mean square (RMS) for each average position in time was then obtained. Only the frequencies between 0.7 and 5 times the heart frequency were considered, in order to reduce the effect of the low-frequency axial movements (such as respiration and head shifts). An upper limit of 5 times the heart frequency was considered because previous studies[9,12] have shown that the ocular tissue movements occur not only at the cardiac frequency but also at its multiple frequencies. In some cases, frequencies up to 7[9] times the cardiac frequency were observed. Nevertheless, in our study, a limit of 5 times the cardiac frequency was chosen in order to reduce the effect of noise on our data. Differences between groups were analyzed using the Mann-Whitney *U* test.

System Characterization

We characterized our system for different parameters in order to evaluate its performance. With a camera exposure time of 30 μs, we could achieve a frame rate of 40 frames per second, where each frame consisted of 720 A-scans with 1250 pixels per A-scan. The scanning mirror was used to steer the beam along a single horizontal line on the retina, centered on the ONH. The experimentally calculated value of the axial resolution which is the minimum distance between the two interfaces in order to see them separately was found to be 8.2 μm in air. For cornea and retina, the axial resolution will be given by the ratio of the axial resolution in air to their respective refractive indices, which gives an axial resolution of 5.96 μm for the cornea, considering a refractive index of 1.376 for the cornea,[13] and 5.94 μm for the retina, considering a refractive index of 1.38 for the retina. The maximum depth range of the system was found to be 3.1 mm in free space. The calibration of the system was performed by moving one reference mirror in steps of 100 μm, and the corresponding FFT peak position was tracked. To estimate the experimental displacement resolution (i.e., the smallest position change that can be measured for a well-resolved peak) of our system, we used a human cadaver eye as a sample. The displacement resolution of an FD-LCI-based system is limited by the noise (such as mechanical and shot noise) present in the system.[14] In order to evaluate the system noise in terms of displacement measurement, the sample eye was mounted on a piezoelectric stage (Piezosystem, Jena, Germany) and moved in sine waveform with amplitudes of 0.5 μm, 1 μm, and 2 μm at 1 Hz. The position of the sample eye cornea was measured, and frequencies lower than 0.7 Hz or higher than 5 Hz were filtered out. A perfect sine wave was fitted to the filtered movement and subtracted to obtain the noise. The standard deviation of the noise was found to be approximately 100 nm. The optical power used on the eye was 500 μW, which is lower than the prescribed limit of 750 μW according to American National Standards Institute (ANSI) standards. The patient's eye was exposed to the light for 20 seconds, during which the patient blinked normally. The average time to align the system in order to make the measurements was less than 1 minute.

Results

The mean age of the glaucoma patients was 66.7 ± 11.6 years, compared to 67.1 ± 10.3 years in the normal group ($P = 0.9$); the mean IOP was 15.6 ± 5.2 mm Hg, compared to 16.9 ± 2.9 mm Hg in the normal group ($P = 0.9$); the mean visual field mean defect was –6.4 ± 6.2 dB, compared to –0.45 ± 0.73 dB in the normal group ($P = 0.02$); and the mean clinical cup to disc ratio was 0.62 ± 0.13, compared to 0.28 ± 0.09 in the normal group ($P = 0.00$). The mean systolic blood pressure was 130 ± 13 mm Hg in the glaucoma group versus 129 ± 13 mm Hg in the normal group ($P = 0.9$), while the mean diastolic blood pressure was 80 ± 9 mm Hg in the glaucoma group versus 83 ± 3 mm Hg in the normal group ($P = 0.3$).

Using the system described above, B-scans (collection of adjacent A-scans along a line) of the cornea at the apex and retina across the optic disc were acquired for 20 consecutive seconds. The B-scan length on the retinal surface was estimated to be approximately 4.7 mm. Out of these B-scans, the longitudinal movement of the cornea at apex, the base of the optic disc cup, and the nasal and temporal peripapillary retina were measured. The locations of these measurement points are shown in Figure 2A. A typical recording of the measured movement is shown in Figure 3. From this figure, it can be seen that different regions of the fundus and cornea

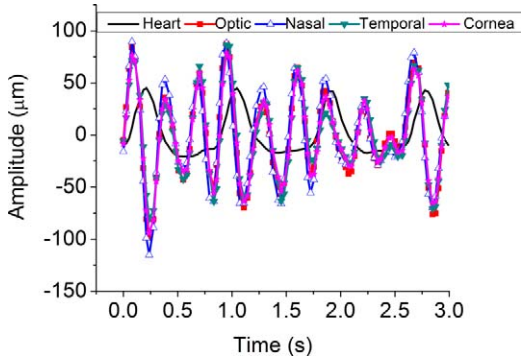

FIGURE 3. The axial movement of the different ocular elements along with the heart cycle is shown. It can be seen that different ocular regions move with a slight difference in amplitude and phase.

move with slightly different amplitudes and phases. Moreover, the ocular tissues pulsate not only with the heart beat but also at its multiple frequencies. Pulsations of the ocular tissues at multiple frequencies of the cardiac cycle have been reported previously by our group,[9] as well as by other groups.[12,15] In order to justify that the observed multiple pulsations are not due to the data processing, a recording of the raw movement of the cornea in a healthy subject is given as Supplementary Figure S1, with the corresponding FFT power spectrum in Supplementary Figure S2 (see Supplementary Material and Supplementary Figs. S1, S2, http://www.iovs.org/lookup/suppl/doi:10.1167/iovs.12-9834/-/DCSupplemental), from which the multiple pulsations in the cornea movement can be clearly seen. The RMS value of the movements of different ocular regions in normal subjects and glaucoma patients is shown in Figure 4 as a solid box plot. In normal subjects, the means ± standard deviations of the RMS value of the movement were found to be 22.7 ± 6.5 μm, 25.4 ± 9.7 μm, 24.8 ± 6.3 μm, and 23.7 ± 7.7 μm for the cornea, base of the optic disc, nasal peripapillary retina, and temporal peripapillary retina, respectively. In glaucoma subjects, the corresponding values were 25.1 ± 8.9 μm, 30.4 ± 11.0 μm, 27.5 ± 10.0 μm, and 27.8 ± 13.4 μm ($P = 0.29$ to 0.52). In the glaucoma

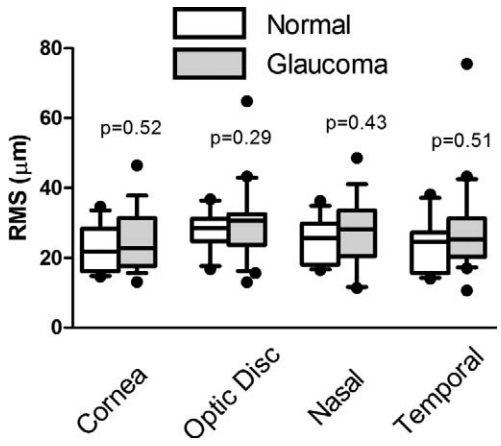

FIGURE 4. The RMS values of the amplitude of axial movement of different ocular regions in normal subjects and glaucoma patients are shown as box plots. The median value is shown in the *center* of the box, while the *top* and *bottom* of the box correspond to the 25th and 75th percentiles, the *whiskers* represent the 10th and 90th percentiles, and the *black dots* at *top* and *bottom* correspond to the outlier values of the distribution. An outlier is any value that is more than 1.5 times the interquartile range from either end of the box.

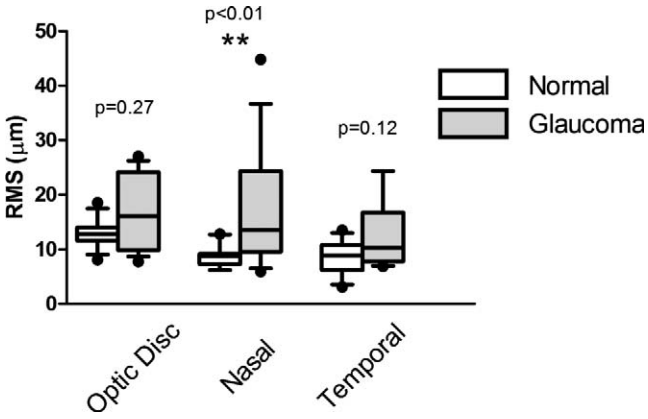

FIGURE 5. RMS value of the amplitude of the FPA at different fundus positions in normal subjects and glaucoma patients. The *black dots* at *top* and *bottom* correspond to the outliers values of the distribution. An outlier is any value that is more than 1.5 times the interquartile range from either end of the box. $^{**}P < 0.01$.

group, the data distribution was skewed toward larger movements. It is interesting to examine the pulsatile expansion of the globe, the fundus pulsation amplitude (FPA), by subtracting the corneal movement from that of the retina or ONH. This process also removes any contribution to these movements from the orbital pulse and was done from the original scans, taking into account the phase differences in these movements. The results are shown in Figure 5. In normal subjects, the mean RMS FPA of the base of the cup was 13.0 ± 2.5 μm, while the same value was 9.0 ± 2.1 μm and 8.7 ± 2.9 μm in the nasal and temporal peripapillary retina, respectively. The corresponding FPA values in the glaucoma group were 16.7 ± 6.8 μm, 17.3 ± 10.9 μm, and 12.7 ± 6.2 μm ($P = 0.26$, $P = 0.008$, and $P = 0.12$, respectively).

Due to amplitude and phase differences in the movements of the different ocular regions, there is local change in the axial distance between different fundus tissues. Since such changes could lead to tissue deformation, we were particularly interested in estimating the local change in distances between adjacent tissues in the optic disc area. By subtracting the absolute position of the peripapillary retina from the position of the base of the ONH cup during the cardiac cycle, we can measure the pulsatile change in the axial distance between the peripapillary retina and the base of the optic disc cup (axial distance between retina and cup [ADRC]). This is done directly

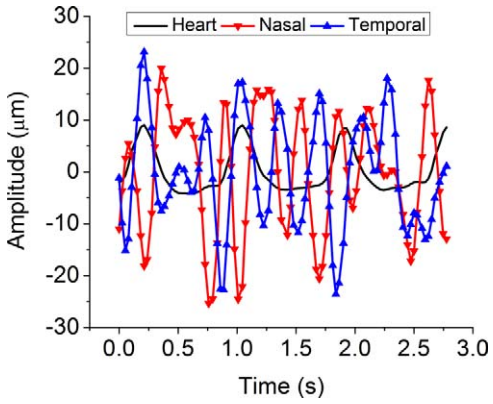

FIGURE 6. Recording of the ADRC change between the base of the optic disc cup and the nasal or temporal peripapillary retina, measured in a healthy volunteer along with the cardiac cycle.

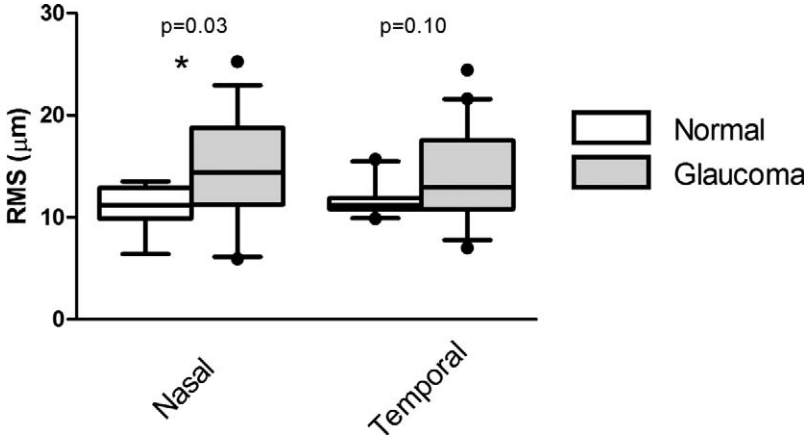

Figure 7. Pulsatile change of ADRC measured on the temporal and nasal side of the optic disc in normal subjects and in glaucoma patients. The ADRC was calculated by subtracting the absolute position of the base of the optic disc cup from the simultaneous position of the temporal or nasal peripapillary retina. The *black dots* at *top* and *bottom* correspond to the outliers values of the distribution. An outlier is any value that is more than 1.5 times the interquartile range from either end of the box. $^{**}P < 0.05$.

from the fundus scans without reference to the cornea. A typical recording of such tissue length change measured in a healthy volunteer is shown in Figure 6. It can be seen from the figure that the ADRC changes during the cardiac cycle on both the nasal and temporal sides of the optic disc. Measurement of the ADRC change during the cardiac cycle is shown in Figure 7, and the means ± standard deviations of the RMS values in normal subjects were found to be 10.7 ± 2.1 μm and 11.6 ± 1.8 μm for the nasal and temporal side of the optic disc, respectively. In the glaucoma patients, the corresponding values were 14.9 ± 5.6 μm ($P = 0.032$) and 14.0 ± 4.9 μm ($P = 0.10$), which on the nasal side were significantly larger than in the normal group. In the glaucoma group, the distribution was skewed toward larger movements. The estimated error on these measurements was found to be less than 1 μm. The process to obtain this error has been described in our earlier work.[9] Briefly, we measured the movement of the retina at 20 consecutive A-scans and subtracted the movement of each A-scan from that of its neighbor. As it can be safely assumed that movement of the retina at neighboring A-scans is the same, the difference in their movements would give an estimation of the error in the measurement, which was less than 1 μm in our case.

Discussion

We measured the elongation during the cardiac cycle of the ADRC and found that the mean RMS elongation during systole was on the order of 11 μm in normal subjects and 15 μm in glaucoma subjects ($P = 0.03$). These data suggest, for the first time, that the nerve fiber layer may actually be deforming over the course of the cardiac cycle. Our primary objective was to establish whether the ADRC changes over the cardiac cycle in normal subjects. We also collected the same data on a group of glaucoma patients, and these data suggest that the ADRC changes are greater in glaucoma patients than in normal subjects. A much larger study of glaucoma patients is underway in order to establish to what degree and in which type of glaucoma patients such pulsatile tissue movements might be significant. The standard deviations of our measurements were much larger in the glaucoma patients than in the normal subjects, with a skew toward large deviations, so it is conceivable that a subgroup of glaucoma patients have much larger tissue deformations than are found in the normal group. It is thought that tissue deformation is one of the main contributors to ONH damage in glaucoma.[4] Our data, then, would be the first suggesting that such deformation occurs in relation to the cardiac cycle.

We also measured the FPA (Fig. 5) and found that the movements measured were greater in glaucoma patients, significantly so in the nasal peripapillary retina. Since FPA measurements are a combination of corneal and fundus movements, they should not be interpreted to reflect only fundus movements. Inasmuch as the corneal movements can be influenced by such factors as ocular elasticity, ocular volume, and choroidal volume, to name a few, the FPA must really be interpreted as a composite of the movement of the cornea and the fundus, an indicator of pulsatile ocular expansion. In contrast, since the ADRC measurement is made solely from the fundus images without reference to the cornea, it is more truly a measurement of fundus tissue movement.

One of the weaknesses of our study relates to the fact that ocular tissues may have different reflectivity in glaucoma than in normal eyes. Such differences could result in different penetration depths and, therefore, different depths of measurement in the two groups. Since we are more interested in movement of tissue than their absolute positions, we do not believe that this issue significantly biases our data, but we hope to be able to look more carefully at this aspect with future technical improvements of our device. Another potential weakness of our study is that, while we corrected for lateral shifts along the beam scanning axis during imaging, we were not able to correct for shifts perpendicular to the axial and the scanning axis. We estimate that, if such shifts were of the same magnitude as our measured horizontal shifts, then their artifactual contribution to z-axis changes would be insignificant. Furthermore, since we impose a frequency filter on the data so as to only consider movements induced by cardiac pulsation, such displacements would have to be occurring at the heart rate to be influencing our measurements.

The tissue movements we observed would result in deformation of these tissues and, possibly, axonal stretching. Most of the literature on axonal stretching in the optic nerve relates to acute traumatic injury. The effect of smaller changes that repeat thousands of times per day and tens of millions of times per year is unknown. If such stretching does play a role, it could be either by a greater amplitude being present or by a greater neuronal susceptibility to stretch in certain individuals. The amplitude of pulsatile tissue movements depends on multiple factors, including the amplitude of vascular pulsa-

tions, the biomechanical properties of the layers of the eye, and the phase difference of movement of adjacent tissues. The fact that most known glaucoma risk factors (as outlined in the introduction) are probably associated with increased ocular pulsatility suggests that this mechanism is worthy of further investigation.

We previously published data suggesting that the base of the optic disc cup moves forward following sustained long-term pressure reduction[16] and that this movement was greater in eyes with thinner corneas,[17] a factor that has been associated with the development and severity of glaucoma.[18] The current study extends the concept of optic disc deformation to a shorter time frame and a more precise anatomical location.

There are certain improvements that will be incorporated in our future studies. First, because of technical limitations, we were only able to make horizontal scans across the ONH. Thus our temporal peripapillary measurements were made at the 9 o'clock position on the right eye, an area that is not as susceptible to early glaucoma damage as the inferotemporal area. It is possible that even larger tissue movements would have been measured in the inferotemporal area, and we are modifying our imaging apparatus in order to investigate this. Second, while we stayed away from areas where large retina vessels were visible, it is possible that some of the movements measured include a component driven by the retinal vasculature rather than the choroid. Even if this is the case, dysynchronous movement of retinal tissue was found which resulted in ADRC changes, and whether these changes were driven by retinal vasculature or choroidal impulses may not be important. Third, our glaucoma group was too small to explore the significance of our findings in a comprehensive way. Our objective here was primarily to present evidence that deformation of retinal tissue might occur at and around the ONH and not to suggest whether such a mechanism is more prominent in glaucoma. The glaucoma data serve to suggest that a larger-scale study of this phenomenon in glaucoma is warranted.

In summary, we present the first evidence that ocular pulsatility may lead to pulsatile ADRC changes and that such changes have a significantly greater amplitude in glaucoma. The role of such movements in ocular pathophysiology remains to be established.

Acknowledgments

The authors thank Leopold Schmetterer for his important input in the development of this device.

References

1. Chang EE, Goldberg JL. Glaucoma 2.0: neuroprotection, neuroregeneration, neuroenhancement. *Ophthalmology*. 2012;119:979–986.
2. Morgan J. Pathogenesis of glaucomatous optic neuropathy. In: Shaarawy TM, Sherwood MB, Crowston JG, Hitchings RA, eds. *Glaucoma: Medical Diagnosis & Therapy*. Vol. 1. Philadelphia: Saunders–Elsevier; 2009:45–54.
3. Leske MC. Open-angle glaucoma—an epidemiologic overview. *Ophthalmic Epidemiol*. 2007;14:166–172.
4. Sigal I, Roberts M, Girard M, Burgoyne C, Downs J. Biomechanical changes of the optic disc. In: Levin LA, Albert DM, eds. *Ocular Disease: Mechanisms and Management*. New York: Elsevier; 2010:153–164.
5. Riva CE, Titze P, Hero M, Petrig BL. Effect of acute decreases of perfusion pressure on choroidal blood flow in humans. *Invest Ophthalmol Vis Sci*. 1997;38:1752–1760.
6. Breusegem C, Fieuws S, Zeyen T, Stalmans I. The effect of trabeculectomy on ocular pulse amplitude. *Invest Ophthalmol Vis Sci*. 2010;51:231–235.
7. Kiss B, Dallinger S, Polak K, Findl O, Eichler H-G, Schmetterer L. Ocular hemodynamics during isometric exercise. *Microvasc Res*. 2001;61:1–13.
8. Schmidl D, Garhofer G, Schmetterer L. The complex interaction between ocular perfusion pressure and ocular blood flow—relevance for glaucoma. *Exp Eye Res*. 2011;93:141–155.
9. Singh K, Dion C, Wajszilber M, Ozaki T, Lesk MR, Costantino S. Measurement of ocular fundus pulsation in healthy subjects using a novel Fourier-domain optical coherence tomography. *Invest Ophthalmol Vis Sci*. 2011;52:8927–8932.
10. Singh K, Dion C, Costantino S, Wajszilber M, Lesk MR, Ozaki T. Development of a novel instrument to measure the pulsatile movement of ocular tissues. *Exp Eye Res* 2010;91:63–68.
11. Wukitsch MW, Petterson MT, Tobler DR, Pologe JA. Pulse oximetry: analysis of theory, technology, and practice. *J Clin Monit Comput*. 1987;4:290–301.
12. Kasprzak H, Iskander DR, Bajraszewski T, Kowalczyk A, Nowak-Szczepanowska W. High accuracy measurement of spectral characteristics of movements of the eye elements. *Opt Pura Apl*. 2007;70:7–11.
13. Atchison DA, Smith G. Refracting components: cornea and lens. In: Atchison DA, Smith G, eds. *Optics of the Human Eye*. Edinburgh: Butterworth-Heinemann; 2000:11–20.
14. Singh K, Dion C, Lesk MR, Ozaki T, Costantino S. Spectral-domain phase microscopy with improved sensitivity using two-dimensional detector arrays. *Rev Sci Instrum*. 2011;82:023706–023704.
15. Kasprzak HT, Iskander DR. Spectral characteristics of longitudinal corneal apex velocities and their relation to the cardiopulmonary system. *Eye*. 2007;21:1212–1219.
16. Lesk MR, Spaeth GL, Azuara-Blanco A, et al. Reversal of optic disc cupping after glaucoma surgery analyzed with a scanning laser tomograph. *Ophthalmology*. 1999;106:1013–1018.
17. Lesk MR, Hafez AS, Descovich D. Relationship between central corneal thickness and changes of optic nerve head topography and blood flow after intraocular pressure reduction in open-angle glaucoma and ocular hypertension. *Arch Ophthalmol*. 2006;124:1568–1572.
18. Gordon MO, Beiser JA, Brandt JD, et al. The Ocular Hypertension Treatment Study: baseline factors that predict the onset of primary open-angle glaucoma. *Arch Ophthalmol*. 2002;120:714–720.